

Modal parameter identification of a containment using ambient vibration measurements

Sanghyun Choi^{a,1}, Sooyong Park^{b,*}, Chang-Hun Hyun^{c,2}, Moon-Soo Kim^{c,3}, Kang-Ryong Choi^{d,4}

^a Department of Railroad Facility Engineering, Korea National Railroad College, 374-18 Woram-dong, Uiwang, Gyeonggi-do 437-763, Republic of Korea

^b Division of Architecture and Ocean Space, Korea Maritime University, Dongsam-dong, Pusan 606-791, Republic of Korea

^c Structural Systems & Site Evaluation Dept., Korea Institute of Nuclear Safety, PO BOX 114, Yuseong, Daejeon 305-600, Republic of Korea

^d Engineering Research Dept., Korea Institute of Nuclear Safety, PO BOX 114, Yuseong, Daejeon 305-600, Republic of Korea

ARTICLE INFO

Article history:

Received 14 December 2008

Received in revised form 20 October 2009

Accepted 12 November 2009

ABSTRACT

Ensuring and maintaining the structural integrity of the containment structure in nuclear power plants is essential for preserving the nuclear reactor and other safety-related systems as well as protecting plant workers and publics from hazardous radioactive materials. To date, the structural integrity of the containment has been evaluated periodically via various nondestructive inspection methods. However, these methods require considerable time and cost to estimate overall structural integrity. In this paper, the possibility of monitoring the structural integrity of the containment utilizing ambient vibration measurement is explored. The ambient vibration testing was selected because it can avoid the interruption of normal operation of power plants. To fulfill the objective, the ambient vibration of the containment of Ulchin Nuclear Power Plant Unit 5 in Korea was measured, and the modal parameters, i.e., resonant frequencies and corresponding mode shapes, were extracted using the modal identification techniques in the frequency domain, i.e., the peak picking and the frequency domain decomposition methods. Using the extracted modal parameters and the finite element model, the elastic modulus of the concrete was estimated based on the sensitivity-based system identification method.

© 2009 Elsevier B.V. All rights reserved.

1. Introduction

As energy needs around the world coupled with rising oil and gas prices along with environmental constraints and concerns about energy supply security persistently grow, the expectations on nuclear energy, which can provide clean and economic energy, rise. According to IAEA (IAEA, 2008), there were 439 nuclear power reactors in operation worldwide by the end of 2007, which provide about 15% of the world's electricity. However, more than 70% of them are more than 20 years old, and thus, assuming the 40 years of design life, majority of the operating nuclear power plants will face decommission or extension of operating licenses. One of the major concerns in extending operating licenses is the integrity of safety-related structures including the containment, since, unlike mechanical and electrical equipments, the replace-

ment of the containment and many other safety-related structures would be economically unfeasible (Naus et al., 1996).

To date, the structural integrity of the containment has been evaluated periodically via visual inspections along with chemical tests, nondestructive strength tests, etc. However, these methods can only provide local information on the structural condition and require considerable time and cost to estimate overall structural integrity (Park and Choi, 2008). One of the more effective methods that have gained attention for evaluating the structural condition of the whole structure is the structural integrity monitoring (SIM) method, which utilizes measured dynamic responses from a structural system to assess the physical properties of the structure (Salawu, 1997; Choi et al., 2006). Usually the SIM method comprises the measurement technique for recording dynamic responses, the data processing technique for extracting dynamic characteristics, e.g., resonant frequencies, damping, and mode shapes, and the system identification technique for relating extracted dynamic characteristics to physical properties of the structural system (Doebbling et al., 1996). For large-scale structures such as high-rise buildings and long-span bridges, measuring dynamic responses appropriately would be the most important task.

There are two test methods available in measuring the dynamic response of a structure: the forced vibration test and ambient vibration test. Until the late 1990s, the forced vibration tests were

* Corresponding author. Tel.: +82 51 410 4588; fax: +82 51 403 8841.

E-mail addresses: schoi86@nate.com (S. Choi), sypark@hhu.ac.kr

(S. Park), k203hch@kins.re.kr (C.-H. Hyun), k181kms@kins.re.kr (M.-S. Kim), k116ckr@kins.re.kr (K.-R. Choi).

¹ Tel.: +82 31 460 4262; fax: +82 31 462 2944.

² Tel.: +82 42 868 0173; fax: +82 42 868 0523.

³ Tel.: +82 42 868 0174; fax: +82 42 868 0523.

⁴ Tel.: +82 42 868 0171; fax: +82 42 868 0523.

preferred due to the accuracy of the corresponding system identification techniques. However, during the last two decades more attention was paid to ambient vibration tests because of their low cost and convenience (Michel et al., 2008). For forced vibration test, a challenging issue is the excitation of large civil engineering structures, which leads to huge reaction mass shakers or impact testing using a falling weight (Peeters et al., 2001). Especially for such a structure as the containment to which applying appropriate excitation is a difficult task, the ambient vibration test is the reasonable choice without interrupting normal operation.

From the pioneering attempt on civil engineering structures in 1930s by Carder (1936, 1937), the ambient test has now become the main experimental method for assessing the dynamic behavior of civil engineering structures in operational conditions worldwide. The main advantages of the ambient vibration test are well summarized by Gentile and Bernardini (2008) as follows:

1. The easy way of testing, which is performed by just measuring the structural response under ambient excitation, usually due to micro-tremors, traffic or wind.
2. The multiple-input nature and the wide-band frequency content of ambient excitation, inducing a significant number of modal contributions in the response.
3. The large number of highly sensitive piezoelectric and force-balanced accelerometers available on the market, especially developed for measurements in the range of 0–100 Hz and relatively inexpensive.
4. The increasing availability of data acquisition and storage systems which are fully computer-based.
5. The large number of robust output-only modal identification techniques available in the literature including the peak picking method (Bendat and Piersol, 1993), the frequency domain decomposition method (Brincker et al., 2000), and the stochastic subspace identification method (Peeters and De Roeck, 1999).

Thus far, the ambient test has been applied to various types of structures including bridges (Magalhães et al., 2009), buildings (Michel et al., 2008), historical structures (Júlio et al., 2008), and mechanical structures (Pierro et al., 2008). However, until now no attention has been focused on the application of the ambient test technique to monitor the structural integrity of the containment. The objective of this paper is to explore the feasibility of applying SIM to containment structures utilizing ambient vibration measurements. In order to achieve the stated objective, the following tasks are performed. First, the ambient vibration of the existing containment structure in operation is measured. Second, the modal parameters including resonant frequencies and corresponding mode shapes are extracted from the measured ambient vibration measurements utilizing the modal identification techniques in the frequency domain, i.e., the peak picking and the frequency domain decomposition methods. Third, a numerical model for the containment structure is constructed and analytical modal parameters are computed. Fourth, the correspondence between the extracted experimental and the analytical modal parameters are established. Finally, the structural parameters of the containment structure are estimated using the identified modal parameters based on the sensitivity-based system identification method.

2. Description of the structure

The structure selected for the aim of this research is the containment of Ulchin Nuclear Power Plant (NPP) Unit 5, located in Kyeongsangbuk-do, South Korea. The containment of the unit, made of reinforced concrete, is composed of a circular base mat,

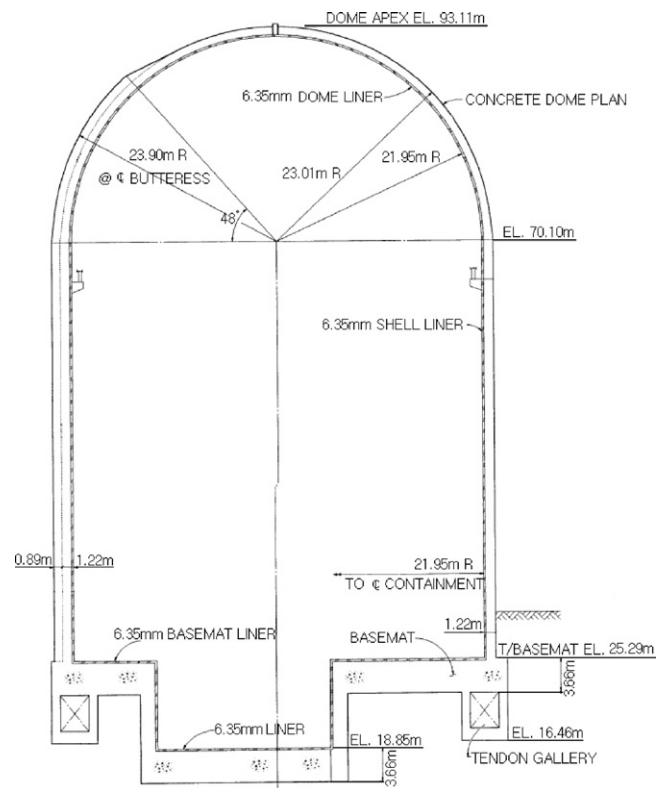


Fig. 1. The cross section of the containment of the Ulchin 5th Unit (KHNP, 2002).

upright cylindrical walls and a spherical-shape dome. The thickness of the cylindrical wall is 1220 mm. The thicknesses of the dome and the base mat are 1070 mm and 3660 mm, respectively. The post-tensioning system with horizontal and vertical tendons is installed in the wall and the dome to secure the containment from cracks and to reinforce the tensile resisting capacity of concrete. The height and the inner diameter of the structure are 67 m and 43.9 m, respectively. On the inner surface of the containment, 6.35 mm thick steel liner plates are installed. The cross section of the containment structure is depicted in Fig. 1. The two neighboring structures, i.e. the primary auxiliary building and the nuclear fuel building, are physically separated with the gaps between the structures filled by chemical substances.

3. Ambient vibration test and numerical modeling

The ambient vibration of the containment of Ulchin NPP Unit 5 under normal operation was measured to explore the feasibility of identifying modal parameters. Acceleration responses of the containment structure were measured using accelerometers mounted to the outer surface of the containment. Also, a finite element model for the containment structure was built to identify the correlation between the experimental and the analytical modal parameters and eventually the structural parameters that control the dynamic behavior of the structure.

3.1. Test setup and procedure

Instrumentation used to conduct the ambient vibration testing consisted of 6 strain-gage-type accelerometers (Fig. 2), a digital dynamic strain meter, an amplifier, and a portable computer (Fig. 3). Data acquisition software installed in the computer was the Visual Log DRA-7630. The length of acquired time window was about 170 min for all datasets. More details on the instru-



Fig. 2. Accelerometers (Tokyo-Sokki ARF-A) mounted on the outer surface of the containment.



Fig. 3. The digital dynamic strain meter, the amplifier, and the computer.

mentation and test settings used for the tests are summarized in Table 1.

Measurement locations representing structural behavior in the modes of interest were chosen to obtain frequency response functions. Since the vertical movement of the containment during the normal operation is negligible comparing to the horizontal movement, only horizontal acceleration responses normal to the outer surface of the containment were measured. The accelerometers were mounted on the outer surface of the containment at 9 locations of the same level (2.7 m above the roof top of the primary auxiliary building and 29.3 m above the basemat) as depicted in Fig. 4. The locations were chosen considering the free vibration analysis results of the structure, the presence of the primary auxiliary building and the nuclear fuel building, and the vertical and horizontal reach limit of a bucket truck. Except Sensors 1 through 5, the other sensors were attached using a bucket truck. Due to the limitation of the number of sensors, the measurements were taken as two separate sets for two days: Set 1 (Sensors 1 through 5) on day one and Set 2 (Sensors 6 through 9) on day two. The reference sensor, at which acceleration responses were measured in both Set 1 and Set 2, was installed between Sensors 1 and 9 and 3 m above other roving sensors. The weather conditions were cloudy with 22 °C on day one and rainy with 21 °C on day two. To minimize the

Table 1
Test parameters.

Parameters	Setting	Units/notes
Sample frequency	50	Hz
Sample length	507,904	Per channel
Accelerometer sensitivity	0.00974	m/s ² /1 μstrain
Accelerometer range	±1.02	g

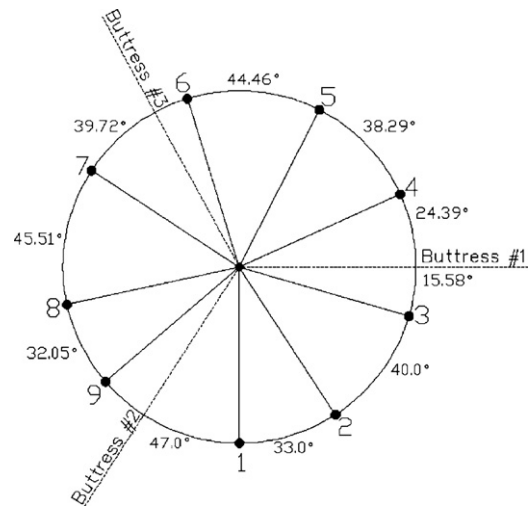


Fig. 4. Sensor locations.

influence of the rain on day two, the sensors were fully wrapped up with watertight tape. The major excitation sources inside the containment were four reactor coolant pumps located about 10 m above the basemat, with a constant rpm of 1190 (19.8 Hz), and four reactor containment fan coolers located about 21 m above the basemat, with a constant rpm of 1200 (20 Hz) and 1800 (30 Hz).

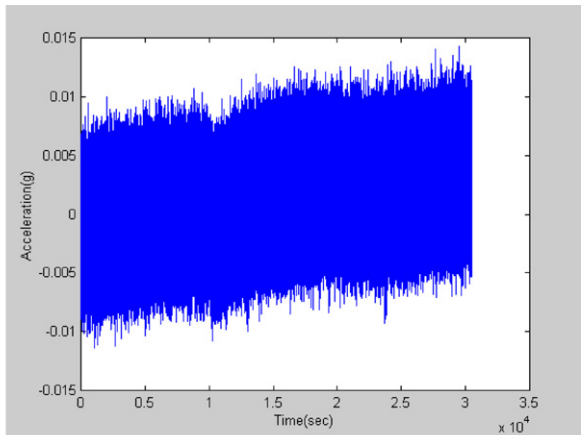
3.2. Identification of modal parameters

The modal parameters were extracted using modal identification techniques in the frequency domain, i.e., the peak picking and the frequency domain decomposition methods. In usual peak picking practice, the transmissibility, which is the ratio of a roving response divided by a fixed reference response for output only modal analysis, is utilized to determine the resonances. However, since peaks in the transmissibility measurement are not the evidence of resonances and thus at least one auto spectrum must be supplemented for locating resonance peaks, the operational deflection shape frequency response function (ODS FRF) is utilized in this paper (Vold et al., 2000). The ODS FRF is formed by combining the magnitude of a roving response auto spectrum with the phase of the cross spectrum between the roving response and the reference response. Unlike the transmissibility, the peaks in the ODS FRF graph represent the resonances. Also, while the transmissibility automatically takes care of the effects of a variable force level between measurement sets, the magnitudes of a set of ODS FRFs must be corrected to account for changes in the excitation level between the measurement sets. The correction can be achieved by multiplying the magnitude of every ODS FRF in the *i*th measurement set by a scale factor, SF_i , defined below:

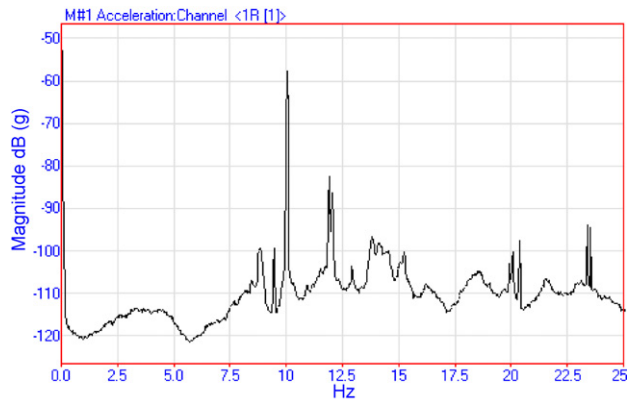
$$SF_i = \sqrt{\frac{\sum_{k=1}^{ns} \bar{S}_k}{ns \cdot \bar{S}_i}} \quad (1)$$

where *ns* is the number of measurement sets and \bar{S}_i is the averaged value of the reference response auto spectrum for the *i*th measurement set.

For the measurements from the containment, the final auto spectrum at each sensor location was calculated via averaging auto spectrums for every 2048 data samples with spectral resolution of 0.0244 Hz. To reduce leakage error, the Hanning window and 50% data overlapping was applied. Fig. 5 shows collected acceleration response and corresponding auto spectrum obtained at Sensor 1. The cross spectrum was computed between each roving (Sensors 1 through 9) and reference measurements. From the ODS FRFs



(a) acceleration response



(b) auto spectrum

Fig. 5. Measured acceleration response and corresponding auto spectrum at Sensor 1.

presented in Fig. 6, three different resonant frequencies were identified as summarized at second column in Table 2. Fig. 7 depicts the configurations of the corresponding mode shapes. Due to the sensor disposition, arranged at one level, only oval modes could be identified.

The frequency domain decomposition (FDD) method consists of decomposing the spectral density matrices into single-degree-of-freedom systems by singular value decomposition (SVD) (Michel et al., 2008). The main procedures for the FDD technique are as follows

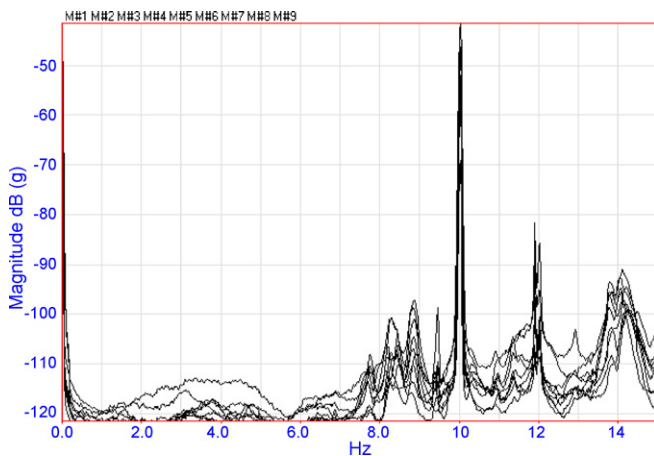


Fig. 6. ODS FRFs for all sensor locations.

Table 2

Resonant frequencies obtained using peak picking and FDD.

Mode	Peak picking	FDD
1	7.715	7.690
2	8.813	8.838
3	10.01	10.01

(Gentile and Bernardini, 2008):

1. Evaluation of the spectral matrix $G(\omega)$, i.e., the matrix in which diagonal terms are auto spectrums while the other terms are cross spectrums;
2. Performing SVD of $G(\omega)$ at each frequency as:

$$G(\omega) = U(\omega)X(\omega)\bar{U}(\omega)^T \quad (2)$$

where the diagonal matrix X collects the real positive singular values in descending order, U is a complex matrix containing the singular vectors as columns, the upper bar denotes the complex conjugate, and the superscript T represents the transpose; and

3. Inspection of the curves representing the singular values to identify the resonant frequencies and estimate the corresponding mode shape using the information contained in the singular vectors of the SVD.

For the measurements from the containment, the spectral matrix was calculated for every 2048 data with 50% data overlapping. The singular values calculated from the spectrum matrix are presented in Fig. 8. From the FDD, three distinct resonant frequencies were identified as summarized at third column in Table 2. In the table, it can be seen that the resonant frequencies extracted by two methods, i.e., the peak picking and the FDD, are almost identical.

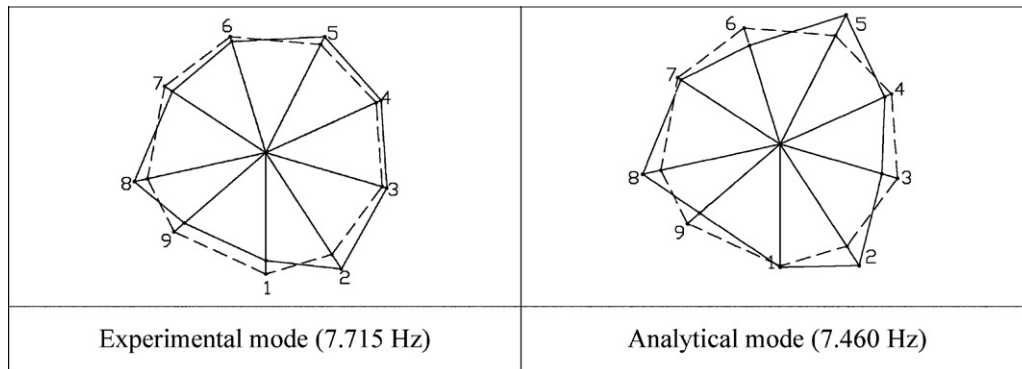
3.3. Numerical modeling

The numerical model of the containment was built using the commercial finite element program ABAQUS (2004). The physical dimensions utilized in modeling the containment are summarized in Table 3. Fig. 9 depicts schematics of the finite element model, tendon profile, and the typical wall model comprised of concrete, reinforcing steels, tendons, and liner plate. The concrete parts of the containment including walls, buttresses, and base mat were modeled using 3-D solid elements. The elastic modulus, the Poisson's ratio, the mass density of the concrete was modeled as 29.5 GPa, 0.17, and 2300 kg/m³ respectively. All the reinforcing steels (yield strength of 420 MPa) were idealized as distributed stiffness in the walls considering spacing, diameters, directions, and locations. The tendons were modeled using truss elements embedded in the walls. The inner steel liners with the yield strength of 224 MPa were modeled using shell elements. The elastic modulus of reinforcing bars and tendons was modeled as 196 GPa and 200 GPa, respectively. The translational movements of the bottom of the basemat were restrained. The free vibration analysis was conducted to obtain the resonant frequencies and the corresponding mode shapes using the

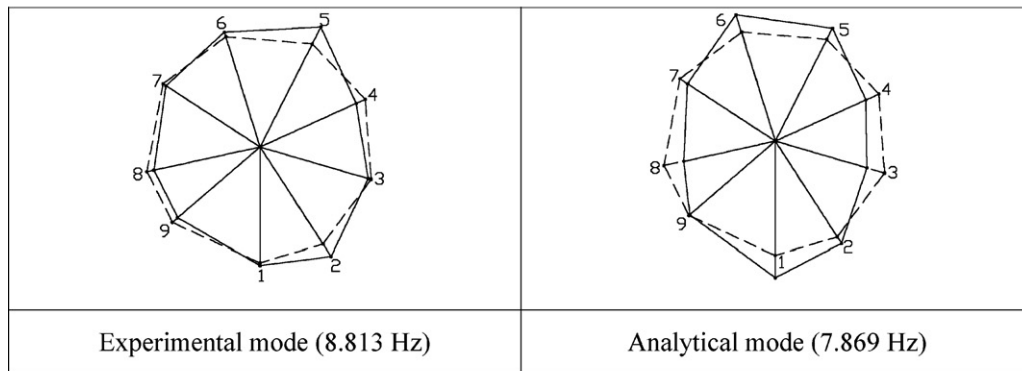
Table 3

Physical dimensions used in modeling the containment.

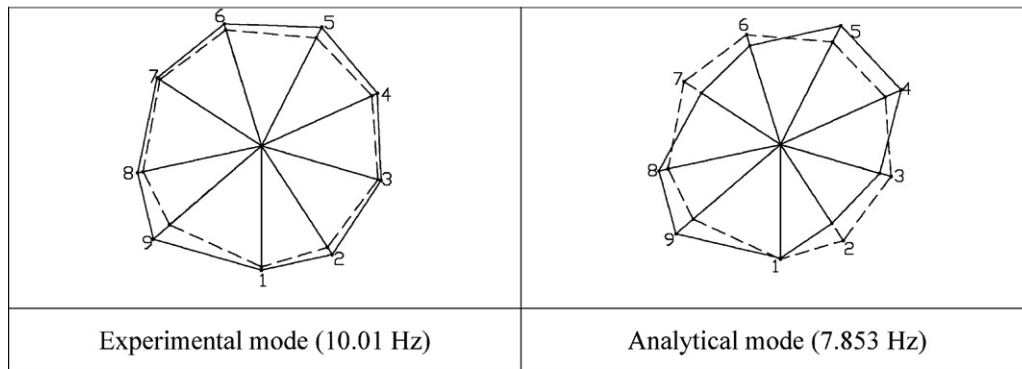
Member		Dimension
Wall	Thickness	1.22 m
	Height	44.81 m
	Inner diameter	43.89 m
Dome	Thickness	1.07 m
	Radius	21.95 m
Buttress	Number	3
	Thickness	2.44 m



(a) mode 1



(b) mode 2



(c) mode 3

Fig. 7. Experimental and analytical mode shapes.

ABAQUS. The analytical mode shapes of the most correspondence with the experimental mode shapes are depicted in Fig. 7.

3.4. Correlation between the experimental and numerical modal parameters

The correspondence between the obtained numerical and the experimental mode shapes can be quantified using the modal assurance criterion (MAC) (Allemang and Brown, 1982).

$$\text{MAC}(\phi_i, \phi_j) = \frac{|\phi_i^T \phi_j|^2}{|\phi_i^T \phi_i| |\phi_j^T \phi_j|} \quad (3)$$

where ϕ_i represents i th mode shape vector. The MAC ranges from 0 to 1; a value of 1 implies perfect correlation of the two mode shapes while a value of 0 indicates uncorrelated mode shapes. In usual practice such as for bridges, if the MAC value between two mode shapes is greater than 80%, the two modes can be considered as closely correlated (Michel et al., 2008). The resulting MAC values are summarized in Table 4. As shown in the table, among three identified modes from the ambient acceleration measurements, considering MAC value of 0.733, the second mode is closely related with the 6th analytical mode while the other two modes show insufficient correlations. The authors attribute poor MAC values obtained for the first and third modes to inevitable errors involved in measuring sensor locations and modeling geometric complexities of the containment as well as the variation in the weather conditions.

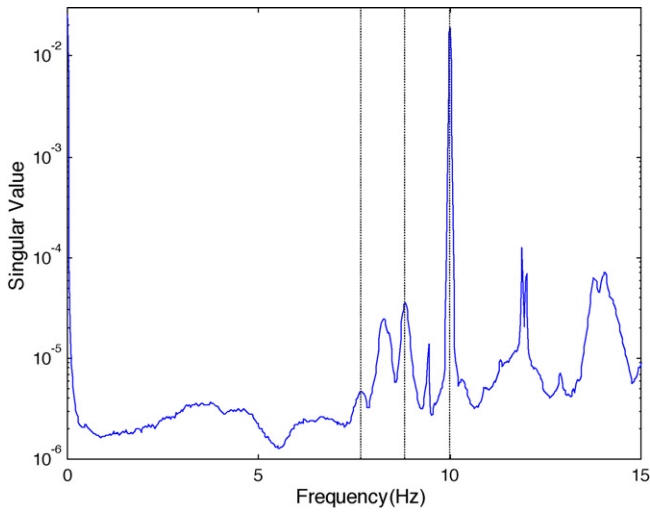


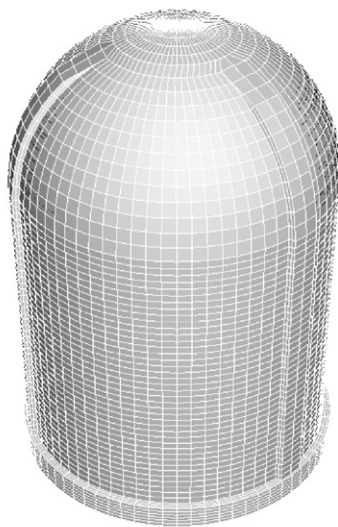
Fig. 8. Singular values of the spectrum matrix.

Table 4
MAC values between the experimental and analytical modes.

Analytical modes (Hz)	Experimental modes (Hz)		
	1 (7.715)	2 (8.813)	3 (10.01)
1 (4.779)	0.212	0.012	0.033
2 (4.779)	0.001	0.004	0.000
3 (7.367)	0.078	0.117	0.057
4 (7.460)	0.449	0.278	0.014
5 (7.853)	0.003	0.000	0.239
6 (7.869)	0.087	0.733	0.001
7 (9.871)	0.138	0.109	0.032

4. System identification

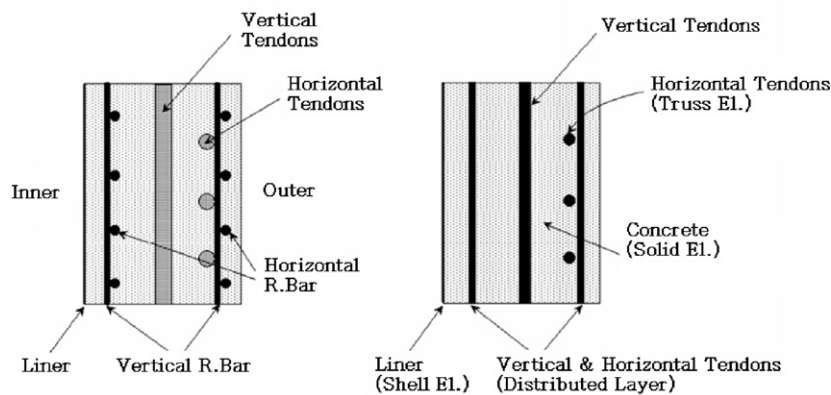
System identification (SI) is defined as the determination, on the basis of input and output, of the characteristics or properties of a system within a specified class of systems to which it is equivalent (Zadeh, 1962). The process of SI consists of three main steps: (1) defining a model and planning some experiments to measure the response of the system (model selection and testing); (2) using the given model and the measured response to estimate the unknown parameters of the model (parameter estimation); and (3) validat-



(a) finite element model for the containment



(b) tendon model



(c) typical wall model

Fig. 9. FE model for the containment.

ing and refining the model (model validation or model updating). In structural mechanics, the parameter estimation has been used to identify the structural parameters and consequently to evaluate the modal parameters (e.g. resonant frequencies, mode shapes, and modal damping) which define the behavior of a structural system. The identified parameters obtained using SI techniques for the structure can then be applied to the problems of nondestructive damage evaluation, and the assessment of structural degradation and deterioration that can reduce the useful life and safety of structures.

To date, many SI methods have been developed based on various theories including time domain procedures (Agbabian et al., 1991), perturbation method (Chen and Wada, 1975), sensitivity-based method (Stubbs, 1985), FRF method (Lin and Ewins, 1994), etc. Imregun and Visser (1991) discussed methods using Lagrange multipliers, perturbation, error matrix, sensitivity, FRF, and statistics, and concluded that sensitivity-based SI techniques, which compute a sensitivity matrix by considering the partial derivatives of modal parameters with respect to structural parameters via a truncated Taylor series expansion, provide a well-updated analytical model capable of reproducing the measured experimental data.

Almost all sensitivity-based methods utilize a sensitivity matrix based on the partial derivatives of modal parameters with respect to structural parameters (Nam et al., 2005). During the identification process, the analytical mass and stiffness matrices of a structural system are updated. An updated eigen solution is obtained and the same process is repeated until the results are satisfied within a predetermined tolerance. It should be noted that the formulation of the sensitivity matrix is based on a truncated Taylor's series expansion and hence the method is an approximate one. In general, sensitivity-type methods depend on the selection of parameters and the definition of the optimization constraints. For instance, the parameters can be elements of the mass and stiffness matrices. A sensitivity-type method that utilizes statistics as the basis for model updating was formulated by Collins et al. (1974) to systematically use experimental measurements of the modal parameters of a structure to modify the stiffness and mass terms of a finite element model of the structure. The sensitivity matrix technique was exploited further in combination with SI and nondestructive damage detection studies by Stubbs and Osegueda (1990a). In this paper, sensitivity-based SI technique developed by Stubbs and Osegueda (1990a) was applied to identify structural parameters of the containment. The effectiveness of the selected method has been verified analytically and experimentally (Stubbs and Osegueda, 1990b; Choi et al., 2004).

4.1. System identification theory

Let the mathematical model of a system be defined by n scalar structural parameters x_i in which $i = 1, 2, \dots, n$, and the parameter, x_i , can be collected into the vector \mathbf{x} . Assuming that $\omega(\mathbf{x} + d\mathbf{x})$ represents the true eigen solutions for a real structural system and that $\omega(\mathbf{x})$ describes the approximate eigen solutions for a mathematical model, using Taylor series expansion the error, ε , can be expressed as:

$$\varepsilon = \omega(\mathbf{x} + d\mathbf{x}) - \omega(\mathbf{x}) = \sum_{i=1}^n \frac{\partial \omega}{\partial x_i} dx_i \quad (4)$$

Normalizing Eq. (4) by dividing by ω_j and rewriting for j th eigen solution, yields:

$$\frac{\varepsilon_j}{\omega_j} = \sum_{i=1}^n \frac{\partial \omega_j}{\partial x_i} \frac{x_i}{\omega_j} \frac{dx_i}{x_i} \quad (5)$$

In matrix form

$$\mathbf{Z} = \mathbf{F}\boldsymbol{\alpha} \quad (6)$$

where the elements of the vectors \mathbf{Z} , representing the j th fractional change of the solution vectors between real and mathematical system, and $\boldsymbol{\alpha}$ the i th fractional changes of the structural parameters, are $Z_j = \varepsilon_j/\omega_j$ and $\alpha_i = dx_i/x_i$, respectively, and the elements of the sensitivity matrix \mathbf{F} are $f_{ji} = (\partial \omega_j / \partial x_i)(x_i/\omega_j)$. The vector $\boldsymbol{\alpha}$ is the only unknown to estimate, e.g., stiffness, mass, or damping. Note that, in this paper, only changes in stiffness parameters are considered in $\boldsymbol{\alpha}$, because in structural parameter identification problems: (1) the change in masses is negligible in common structural damage (e.g., cracks, time-dependent stiffness degradation in concrete structure, delamination in composite structures, loosen connections in steel structures); and (2) the effect of changes in damping parameters on changes in spectral information (e.g., natural frequencies) is negligibly small (Farrar and Jauregui, 1996). It should be noted that the solution obtained by Eq. (6) is the minimal norm solution and may not be unique.

Suppose that the corresponding sets of m resonant frequencies of the initial FE model and the existing structure are known. Before implementing Eq. (6) to get the fractional stiffness changes of n elements between the initial and the existing structures, the sensitivity matrix, \mathbf{F} , should first be developed. The following procedure can be used to determine the sensitivity matrix: first, m resonant frequencies are numerically generated for the initial FE model of a system; second, a known fractional stiffness change, α_j at element j of the FE model is introduced and the corresponding m resonant frequencies are numerically generated; third, the fractional changes between the m initial frequencies and the m frequencies corresponding to the parameter α_j are computed; fourth, each component of the j th column of the matrix \mathbf{F} is computed dividing the fractional changes in each frequency by the simulated severity at the element j ; and finally, the $m \times n$ matrix \mathbf{F} is generated repeating the procedure for all n elements. With the \mathbf{F} matrix obtained, the following 7-step algorithm is proposed to identify a target structure:

1. Extract FRFs and natural frequencies from the target structure (i.e., an existing structure).
2. Select an initial FE model of the structure utilizing all possible knowledge about the design and construction of the structure.
3. Compute the natural frequencies of the initial FE model.
4. Compute the sensitivity matrix, \mathbf{F} , for the FE model.
5. Compute the fractional changes in frequencies between the FE model and the target structure.
6. Fine-tune the FE model by first solving Eq. (6) to estimate stiffness changes and consequently to update stiffness parameters of the FE model.
7. Repeat steps 1–6 until $\mathbf{Z} \approx 0$ or $\boldsymbol{\alpha} \approx 0$ when the structural parameters of the FE model are identical to the existing target structure.

4.2. System identification results

The identification procedure consisted of the following three steps: (1) assume an initial set of physical parameter values for the FE model based on the information about design reports, test results, etc.; (2) generate sensitivities of the eigen solutions to the physical parameters using the FE model; and (3) update the physical properties of the FE model using the procedure outlined in the preceding section. In the first step of the SI process, assuming that the changes in other stiffness parameters were relatively small, the authors selected the elastic modulus of the concrete for the stiffness parameter to be identified because only one resonant frequency with acceptable correlation was available. The initial elastic modulus of the concrete was set 29.5 GPa based on the design data. The

sensitivity of the selected physical property of the structure to the eigen solution, i.e., the 6th mode based on the correlation study presented in Table 4, was established using the finite element model described in Section 3.3.

Using the computed sensitivity, the measured frequency, and the numerical model, the elastic modulus of the concrete was estimated as 37 GPa, which is 25% greater than the initial value. Taking into account the results from the initial strength test of the concrete utilized for the construction of Ulchin NPP Unit 5, in which the elastic modulus of the concrete was estimated approximately 10% greater than the design value, the usual long term strengthening characteristics of the concrete (Park and Paulay, 1975), and the presence of the prestressing system, the identification result can be considered reasonable.

5. Conclusions

In this paper, the ambient vibration measurements from the containment of Ulchin NPP Unit 5 and the modal parameters, i.e., resonant frequencies and corresponding mode shapes, extracted using the modal identification techniques in the frequency domain, i.e., the peak picking and the frequency domain decomposition methods, were presented. Based on the extracted modal parameters and the finite element model constructed for the containment, the elastic modulus of the concrete was estimated using the sensitivity-based system identification method. From the study, the following conclusions are drawn:

1. From the ambient vibration measurements, resonant frequencies along with corresponding mode shapes can be extracted using the frequency domain modal identification techniques;
2. the correlations between the experimental and analytical mode shapes of the containment are identified via the MAC, and one mode shows acceptable correlation;
3. in measuring the ambient vibration of the containment, more corroborated efforts are needed to enhance the accuracy of the identified modal parameters;
4. the elastic modulus of the concrete is estimated using the sensitivity-based SI method and the obtained value is approximately 25% greater than the design assumption; and
5. using the ambient vibration measuring techniques along with the modal identification techniques and the SI methods, the structural integrity of the containment can be monitored without interrupting normal operation.

Acknowledgements

This research was supported by the Korea Institute of Nuclear Safety (Contract Number RS05-56-PB). The authors also thank Korea Hydro & Nuclear Power Co. and Daewoo Institute of Construction Technology Co. for their supports and cooperation in modal testing and analyzing the containment of Ulchin NPP Unit 5.

References

ABAQUS Version 6.5, 2004. User's Manual. Hibbitt, Karlsson & Sorensen Inc., Providence.

Agbalian, M.S., Masri, S.F., Miller, R.K., Caughey, T.K., 1991. System identification approach to detection of structural changes. *ASCE J. Eng. Mech.* 117 (2), 370–390.

Allemang, R.J., Brown, D.L., 1982. A correlation coefficient for modal vector analysis. In: *Proc. 1st Int. Modal Analysis Conf. (IMAC)*, Orlando, FL.

Bendat, J.S., Piersol, A.G., 1993. *Engineering Applications of Correlation and Spectral Analysis*. Wiley Interscience, New York.

Brincker, R., Zhang, L., Anderson, P., 2000. Modal identification from ambient responses using frequency domain decomposition. In: *Proc. 18th Int. Modal Analysis Conf. (IMAC)*, San Antonio, TX.

Carder, D.S., 1936. Observed vibration of buildings. *Bull. Seismol. Soc. Am.* 26, 245–277.

Carder, D.S., 1937. Observed vibration of bridges. *Bull. Seismol. Soc. Am.* 27, 269–289.

Chen, J.C., Wada, B.K., 1975. Criteria for analysis–test correlation of structural dynamic systems. *J. Appl. Mech.* 6, 471–477.

Choi, S., Park, S., Bolton, R., Stubbs, N., Sikorsky, C., 2004. Periodic monitoring of physical changes in a concrete box-girder bridge. *J. Sound Vib.* 278, 365–381.

Choi, S., Park, S., Park, N.-H., Stubbs, N., 2006. Improved fault quantification for a plate structure. *J. Sound Vib.* 297, 865–879.

Collins, J.D., Hart, G.C., Hasselman, T.K., Kennedy, B., 1974. Statistical identification of structures. *AIAA J.* 12 (2), 185–190.

Doebbling, S.W., Farrar, C., Prime, M.B., Shevitz, D.W., 1996. *Damage Identification and Health Monitoring of Structural and Mechanical Systems from Changes in their Vibrational Characteristics: A Literature Review*. Los Alamos National Laboratory, LA-13070-MS.

Farrar, C., Jauregui, D., 1996. Damage detection algorithms applied to experimental and numerical modal data from the I-40 bridge. Technical Report LA-13074-MS. Los Alamos National Laboratory.

Gentile, C., Bernardini, G., 2008. Output-only modal identification of a reinforced concrete bridge from radar-based measurements. *NDT E. Int.* 41, 544–553.

IAEA, July 2008. *Nuclear Technology Review 2008*. GC(52)/INF/3.

Imregun, M., Visser, W.J., 1991. A review of model updating techniques. *Shock Vib. Dig.* 23 (1), 9–20.

Júlio, E.N.B.S., da Silva Rebelo, C.A., Dias-da-Costa, D.A.S.G., 2008. Structural assessment of the tower of the tower of the University of Coimbra by modal identification. *Eng. Str.* 30, 3468–3477.

Korea Hydro and Nuclear Power (KHNP), 2002. *Final Safety Analysis Report for Ulchin Unit 5 and 6*. Daejeon, Korea.

Lin, R.M., Ewins, D.J., 1994. Analytical model improvement using frequency response functions. *Mech. Syst. Sig. Proc.* 8 (4), 437–458.

Magalhães, F., Cunha, Á., Cartano, E., 2009. Online automatic identification of the modal parameters of a long span arch bridge. *Mech. Syst. Signal Proc.* 23, 316–329.

Michel, C., Guéguen, P., Bard, P.-Y., 2008. Dynamic parameters of structures extracted from ambient vibration measurements: an aid for the seismic vulnerability assessment of existing buildings in moderate seismic hazard regions. *Soil Dyn. Earth Eng.* 28, 593–604.

Nam, D., Choi, S., Park, S., Stubbs, N., 2005. Improved parameter identification using additional spectral information. *Int. J. Solids Str.* 42, 4971–4987.

Naus, D.J., Oland, C.B., Ellingwood, B.R., Graves III, H.L., Norris, W.E., 1996. Aging management of containment structures in nuclear power plants. *Nuclear Eng. Des.* 166, 367–379.

Park, S., Choi, S., December 2008. Development of methodology for estimating the effective properties of containment buildings. Mid-term Report. Korea Institute of Nuclear Safety, KINS/HR-836.

Park, R., Paulay, T., 1975. *Reinforced Concrete Structures*. Wiley, New York.

Peeters, B., Maeck, J., De Roeck, G., 2001. Vibration-based damage detection in civil engineering: excitation sources and temperature effects. *Smart Mater. Str.* 10, 518–527.

Peeters, B., De Roeck, G., 1999. Reference-based stochastic subspace identification for output-only modal analysis. *Mech. Syst. Signal Proc.* 13 (6), 855–878.

Pierro, E., Mucchi, E., Soria, L., Vecchio, A., 2008. On the vibro-acoustical operational modal analysis of a helicopter cabin. *Mech. Syst. Sig.*, doi:10.1016/j.ymsp.2008.10.009.

Salawu, O.S., 1997. Detection of structural damage through changes in frequency: a review. *Eng. Mech.* 19 (9), 718–723.

Stubbs, N., 1985. A general theory of non-destructive damage detection in structures. In: Leipholz, H.H.H. (Ed.), *Structural Control*. Martinus Nijhoff Publishers, Dordrecht, The Netherlands, pp. 694–713.

Stubbs, N., Osegueda, R., 1990a. Global non-destructive damage evaluation in solids. *Int. J. Analyt. Exp. Modal Anal.* 5 (2), 67–79.

Stubbs, N., Osegueda, R., 1990b. Global damage detection in solids—experimental verification. *Int. J. Analyt. Exp. Modal Anal.* 5 (2), 81–97.

Vold, H., Schwarz, B., Richardson, M., 2000. Measuring operating deflection shapes under non-stationary conditions. In: *Proc. 18th Int. Modal Analysis Conf. (IMAC)*, San Antonio, TX.

Zadeh, L.A., 1962. From circuit theory to system theory. *Proc. IRE.* 50, 856–865.